Received: 31 July 2023 | *Revised:* 8 September 2023 | *Accepted:* 3 January 2024
DOI: 10.37917/ijeee.22.1.1 *Vol. 22 | Issue 1 | June 2026*

Iraqi Journal for Electrical and Electronic Engineering
Original Article

Open Access
IJEEE University of Basrah College of Engineering

Denoising Techniques to Enhance P300 Signal Application of Lie Detection Technology Based-on EEG

Ali Rifaat Abd Almonim*, Anas L. Mahmood
Electronic and Communications Engineering, Al-Nahrain University, Baghdad, Iraq

Correspondance
*Ali Rifaat Abd Almonim
Electronic and Communications Engineering, Al-Nahrain University, Baghdad, Iraq
Email: alialanizy00@gmail.com

Abstract
In recent years, there has been a lot of interest in the study of P300 potential-based approaches for lie detection. The variations in brain signal activity (EEG-P300 component) that distinguish between lying and starting the truth are investigated. As soon as participants respond to an experiment stimulus for the first time, their brain signals are examined and the P300 signal is extracted. This paper aims to improve the signal-to-noise ratio (SNR) of P300, which leads to an increase in the classification accuracy of lie detection. Ten subjects were randomly assigned to groups of lying and innocent people, and 14 electrodes captured the EEG data for each group. This work proposed to use some denoising techniques like averaging the raw EEG signal, regression-based baseline correction, and independent component analysis (ICA). The suggested approach and other early published methods vary mostly in the regression-based technique used in bassline correction to adaptively indicate the baseline interval (baseline window). Compared to other studies, the suggested technique gives an increase in the mean amount of SNR by up to 20% was obtained.

Keywords
Electroencephalogram (EEG), Artifacts, Signal-to-noise Ratio (SNR), Lie Detection.

I. Introduction

The scientific society has recently shown a lot of interest in identifying falsehoods using various techniques. A polygraph, which gauges the reaction of the autonomic nervous system, is an existent tool for lie detection. However, it varies significantly in terms of accuracy and authenticity depending on the type of investigation. Subjects can control their physiological reactions such as keeping quiet and training to lie without any nerve reaction, making it hard to tell certainly whether the person is lying or not [1]. Brain signals are utilized to recognize hidden information in the brain and detect lies as a solution to this issue. As it is not possible to control the brain signals that are produced by the response to a particular stimulus [2].

Electroencephalography (EEG), functional Magnetic Resonance Imaging(fMRI), and functional Near-Infrared Spectroscopy (fNIRS) are a few commonly utilized methods that exhibit benefits in lie detection [3]. The EEG technique is the most popular one [1]. The EEG method is mostly used to monitor and diagnose epilepsy, stroke, seizures, or sleep problems in medicine. The EEG approach offers a wider range of applications, such as in security, entertainment, and communication and Brain-Computer Interfaces (BCI). Machine learning techniques [4] [5] [6], bootstrapped amplitude difference (BAD) [7] [8], and bootstrapped correlation difference (BCD) [9] are three broad categories into which popular P300-based lie detection approaches may be generally subdivided. Three different types of stimuli, referred to as Probe (P), Target (T), and Irrelevant (I) stimuli, are provided to subjects using the methods described above. To obtain the highest level of accuracy, an effective lie detection technique should only require a few stimuli. One of the most important steps necessary to achieve this goal is to extract the P300 with the lowest possible noise and this is possible when the SNR ratio is increased even though the P300 occurs at a constant phase time with stimulus and a complex noise overlapping with

raw EEG signal [10]. The statistical method of bootstrapping is used by BAD and BCD to produce many Event-Related potentials (ERP) averages from the same set of stimuli [4]. Bootstrapping can be used to boost the SNR of P300. Such a move would also cause the subjects to become more exhausted since it would require more time to acquire the signal because it involves so many stimuli. In addition, many researchers have found different ways to achieve lie detection by machine learning with a single trial [3]. In many cases, attention is paid to detecting lies from a single trial without focusing on the effect of noise on the signal on the accuracy of detection, especially when using a smaller number of trials.

The noise present in individual P300 extraction experiments can be considered as follows. There are two basic components to the EEG recording on a single sensor. Extra-skull noise makes up one portion, While the signals output by neurons within the skull in defective areas of the human brain affect the recording of EEG and Event-Related Potential (ERP). The sensor's signal cannot directly represent the ERP. Because P300's time courses and scalp projections typically overlap with noise and spontaneous EEG. conventional denoising techniques (like traditional baseline correction) were unable to distinguish between them precisely. Baseline correction is a crucial pre-processing method used, for example, in 2D gel electrophoresis, to distinguish actual spectroscopic signals from interference effects or eliminate the background effect of the signal. It is a key topic in both historical and contemporary methodological discussions in ERP research, serving as a possible substitute for robust high-pass filtering. However, the signal-to-noise ratio is implied to decrease by the very assumptions that underlie traditional baseline. So, statistically speaking, traditional baseline correction is not only unneeded but also undesirable. In a GLM (General Linear Model) -based statistical technique, in this method, the predictor is used to find the baseline period for which the data is an input to find the required baseline correction period [11]. This will reduce backward error dispersal by enhancing statistical power. This technique is called regression-based baseline correction.

Later, to obtain the independent components (ICs) of the stimulus-associated ERP, independent components analysis (ICA) is used. The results showed that the ICs are clearer to the extent that they can be distinguished more than the raw signals from the sensors [12]. A previous study suggested the topography-template matching (TTM) algorithm, an ICA-based template matching technique, to improve the P300-EEG SNR, and it showed encouraging returns [12]. The core of the innovation is how the P300's independent components are automatically identified [13]. Resting-state EEG can be analyzed in terms of its physiological characteristics when appropriate complex algorithms are used on pre-processed signals. With actual values of ICA applied to the waveforms in the time domain, this demonstrates the value of ICA for EEG analysis, identification, and removal of artifacts. [14].

Since information transmission by neurons is a noisy stochastic process, using the SNR to describe the fidelity of neural systems is intriguing. However, since neurons transmit both signal and noise predominantly in their action potentials, which are binary electrical discharges also known as spikes, the usual idea of SNR cannot be used in neural analysis [15]. The effect on the signal-to-noise ratio of different preprocessing techniques is evaluated. The signal-to-noise ratio (SNR) was defined as the ratio between the mean signal amplitude (evoked field) and the standard error of the mean over trials. The goal of the current study was to describe the change in signal-to-noise ratio (SNR) following the use of the most popular artifact identification and artifact reduction techniques during the preprocessing of EEG data. The SNR has been used in the past to rate preprocessing quality. [16].

II. Experimental Protocol

In this investigation, the common three-stimuli procedure was used [17]. The subjects were separated into two groups at random: a lying-free group and a lying group. Six distinct coins were attended, and the images of them served as detection stimuli. Each subject received a box including one or two coins for the lying-free and lying groups respectively. They were told to open the box and take notes on the contents. The experiment started by giving the false group some instructions to steal one of the coins from the box and this coin will be a trigger for the probe (P) stimulus. The remaining four images were irrelevant (I) stimuli, whereas the other item in the box that which left without stealing was the target (T) stimulus. The box's contents were not stolen from the lying-free subjects, therefore that was the T stimulus. Each participant was given instructions to record details about the items in the box, such as the value and colors (bronze, silver, or gold) of the coins. Following the completion of the above-mentioned beginning activities, the subjects started the process. subjects were sitting one meter away from a screen showing a video. This video shows pictures of stimuli P, I, and T randomly. Every piece remained for half a second and 20 iterations through one session, this took three minutes, including a minute of break. The stimulus interval lasted 1.6 seconds. Any subject possesses five sessions to complete. Fig. 1 shows the stimulus sequence graph. Each participant was given a push button, and when presented with known and unfamiliar objects, they were ordered to push the "Yes" or "No" buttons, respectively. When presented with the target and irrelevant stimuli, the lying group was told to push the "Yes" or "No" buttons, respectively. They were instructed to click the "No" button in response to a P stimulus to cover up

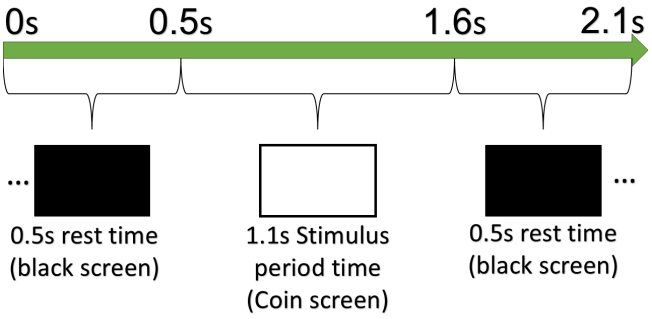

Fig. 1. The diagram of the stimulus

the theft. The lying-free group, on the other hand, responded truthfully to every stimulus. None of the subjects intended to eliminate those with more than a 5% clicking error—fit this description. Finally, Fig. 2 presents a rough map to explain the process mentioned above.

III. Proposed Methodology

The suggested approach is created in this part to get over the noise impact and provide a reconstructed waveform with greater SNR for better ERP P300 component categorization. Fig. 3 provides a logical overview of the suggested approach. This section describes the details of the proposed technique used in this paper.

A. Data Acquisition

As shown in Fig. 4 twelve electrodes from the International 10-20 system (Fp1, Fp2, F3, FZ, F4, C3, CZ, P3, PZ, and Oz) were employed. The signal resulting from eye movement or blinking is recorded from two places near the eye. The first is called horizontal Electrooculography (EOG), which is taken near the corner of the eye (canthus), and the second is the vertical EOG, which is taken a few millimeters above or below the right eye. EEG and EOG data were digitalized at 500 Hz using "Nic Vue" (the software of Nicolet EEG v32 device) and filtered using a band pass filter live at 0.1–30 Hz. The right earlobe served as the reference point for each electrode.

B. Epochs Raw Data

A data structure called epochs objects is used to represent and analyze equal-duration segments of the EEG signal as shown in Fig. 5. Epochs can also be used to store sequential or overlapping frames of a continuous signal, although they are most frequently employed to represent data that is time-locked to recurrent experimental events (such as stimulus onsets or subject button pushes). In Fig. 5 the EEG signals are taken from 12 electrodes arranged on the Y-axis from Oz to Fp1.

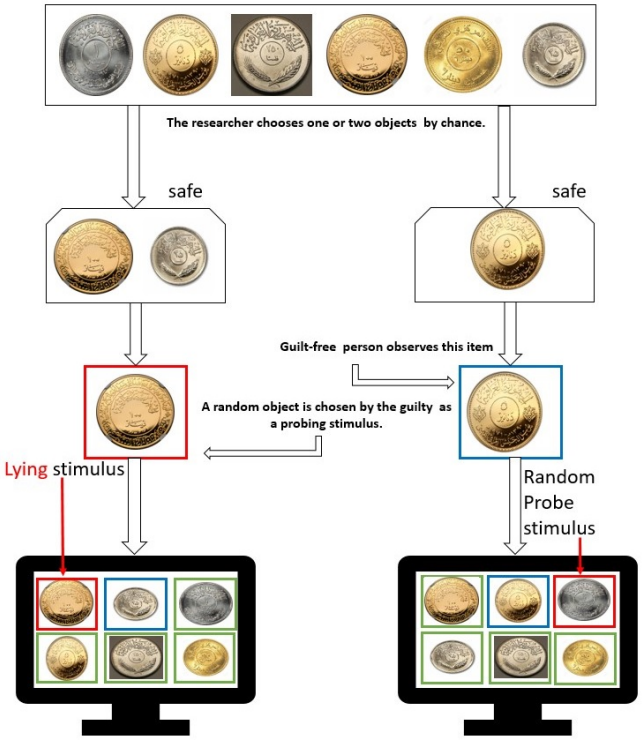

Fig. 2. Experiment scenario

The EEG signals are divided into epochs everyone starts 0.5 s before and 1.1 s after the stimulus.

C. Discard Datasets Excessed ±75 Microvolts (μv)

The automated rejection mechanism, for example, based on the peak-to-peak signal, is a popular method for rejecting problematic epochs. The corresponding EEG epoch may be regarded as a poor trial and excluded from the analysis if the peak-to-peak amplitude in the EEG data exceeds a predetermined threshold.

D. Regression-based Baseline Correction

In this work, this technique solves a main problem that occurs when using baseline correction in ERP (Event-Related-Potential) research which is the choice of the baseline period and the supposition that there are no systematically different conditions during the baseline interval. We'll illustrate that regardless of the baseline period or high-pass filter configuration, the classic baseline correction is never the best strategy for employing new statistical approaches. In brief, to remove any bias caused by signal drifts, adding the baseline time frame to the statistical computation is the right plan of action. Equation (1) represents generally linear modeling (GLM) as in,

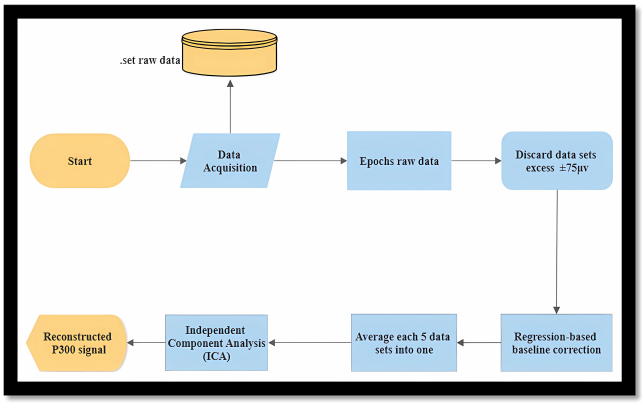

Fig. 3. Proposed model to reconstruct the p300 signal

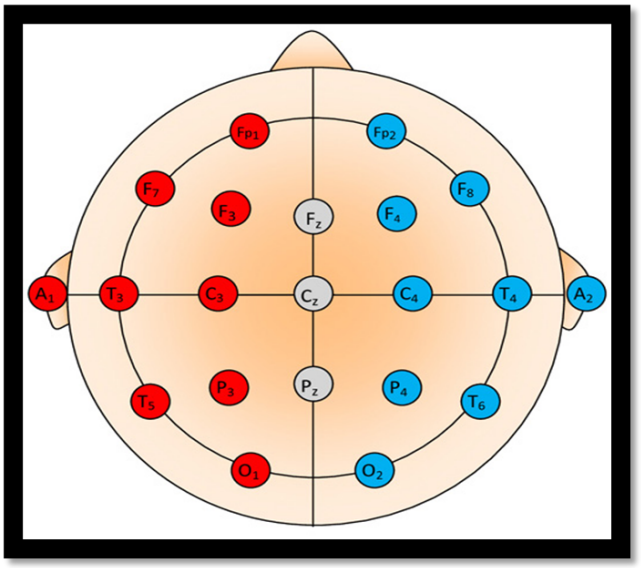

Fig. 4. Top view of the head to clarify electrode locations based on (10-20 system of electrode placement)

$$Z = \sum_{j \in \text{covariates}} \delta_j X_j + \varepsilon \tag{1}$$

- z: column vector of EEG data.
- X_j: column vectors representing different predictors and covariates.
- δ_j: represents the weights of X_j (statistically calculated).
- ε: represents the error term.

In baseline-corrected analyses of statistics, the z column can be analyzed into the following equation:

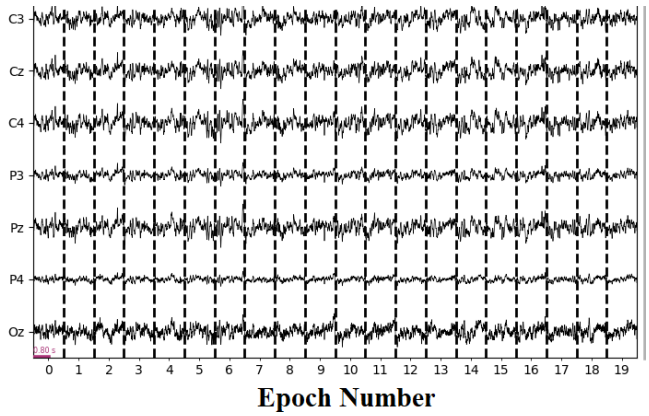

Fig. 5. Epochs of the raw EEG dataset

$$Z = Z_{\text{window}} - Z_{\text{baseline}} \tag{2}$$

It is not necessary to specify the removal of the baseline from the epoch before or after averaging over a fixed time range. This is due to the baseline adjustment being constant for a particular epoch and the average difference being equal to the variation from the average. This study may thus regenerate GLM as (3) shown below

$$Z_{\text{window}} - Z_{\text{baseline}} = \sum_{j \in \text{covariates}} \delta_j X_j + \varepsilon \tag{3}$$

which may change to read as (4)

$$z_{\text{window}} = \sum_{j \in \text{covariates}} \delta_j X_j + z_{\text{baseline}} + \varepsilon \tag{4}$$

practically, this study noticed that this is essential when understanding biasing. Traditional baseline correction always shifts the inverse biasing of signals at all electrodes into the epoch, while the regression-based approach's weighting effectively corrects for this biasing rather than coercively moving it. There are two methods to do this. Firstly, the baseline window's weighting might vary depending on the electrodes. Second, the baseline window's weighting might vary depending on the conditions. The baseline correction can be applied individually to each electrode or condition (as in traditional baseline correction) or the effects of interaction for topographic location or condition can be included in the regression model. Many of the biases that exist in the signals may be avoided by using such appropriate statistical control. This research demonstrates that traditional baseline correction can be deceptive in certain situations, but the regression-based method effectively accounts for biasing changes in the baseline conditions.

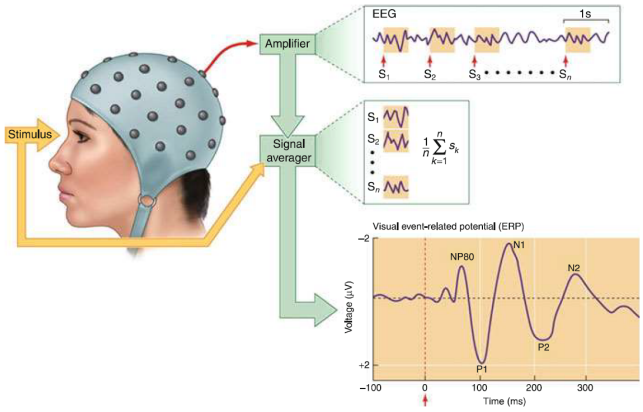

Fig. 6. ERP generated by averaging the EEG signals of many stimuli (S1, S2, S3, ..., Sn) at brain response to an image stimulus.

E. ERP Configuration of EEG Signals

The stimulus-response P, I, and T datasets were chosen, and 5 datasets from each subject were combined to create an average. The averaging process aims to improve the signal-to-noise ratio (SNR) and produce the evoked EEG signal, also called the ERP signal [18]. Fig. 6 shows the effect of the increased number of trials and subjects on the averaging process.

F. Independent Component Analysis (ICA)

There are several methods for fixing artifacts moreover, a few artifact repair tools are included in the MNE-Python library inclusive digital filtering, signal-space separation (SSS)/Maxwell filtering, signal-space projection (SSP), and independent components analysis (ICA) [19] [20]. Many artifact correction methods apply to both continuous (raw) data and already-epoch data. Of course, you must first find the artifacts to select any of these methods that can use. In this work, the overlapping of the EOG and EEG signals in the time and frequency domains causes the ocular artifacts. (ICA) is a method for determining the independent source signals from a collection of recordings when the source signals were mixed in an unknown ratio. Fastica, Picard, and Infomax are the three distinct ICA algorithms. Picard is a discovery method that is anticipated to converge more quickly than FastICA and Infomax [13] [21]. Picard was to be more resilient than other algorithms in situations when the sources are not entirely independent, as is frequently the case with actual EEG data. Before executing the ICA decomposition, the data are generally scaled to unit variance and whitened using principal components analysis (PCA). Fig. 7 summarizes the fitting and reconstruction processes (by using the MNE-python library) as well as the variables that affect dimensionality at different stages [22].

G. Signal-To-Noise Ratio (SNR)

The ratio between the mean signal amplitude of the interest region as shown in (5) (evoked field) and the standard error of the mean of noise region as shown across trials as shown in (6) was called the signal-to-noise ratio (SNR) as shown in (7). Identify the regions of interest in the ERP waveform that contain the signal (at this work 0.5s to 1.6s) and the regions that represent noise (-0.5s to 0.5s). The signal region typically corresponds to the ERP component of interest, while the noise region may include the baseline or pre-stimulus activity [16].

$$\bar{s} = \frac{1}{N}\sum_{i=1}^{N} s_i \tag{5}$$

$$\delta = \sqrt{\left(\frac{\sum_{i=1}^{N}(s_i - \bar{s})^2}{N}\right)} \tag{6}$$

$$\text{SNR} = \frac{\bar{s}}{\delta} \tag{7}$$

where $\bar{s}$ is the signal average (event-related potential) across epochs, δ is the standard error across epochs, and N is the number of epochs.

IV. Experimental Results

As noted previously in the introductory section, the P300 response, which is maximal at the parietal lobe Pz, intermediate at Cz, and smallest at Fz, is the major focus of the research on ERP. Fig. 8 demonstrates the difference in amplitude of these channels. As a result of the step that deletes the bad epochs as in Fig. 9 notice that regarding the Pz channel, it is less noisy, as the peak-to-peak amplitude did not exceed ±75 μv in all epochs. Fig. 10 shows the compression between the ERP P300 signal that is used in lie detection without baseline correction, with traditional baseline correction (other researchers used), and with regression-based baseline correction. At Fig. 10 a and b noticed that the channel signals of a lying group are shifted down and up causing the p300 sample uncleared because of the noise effect and choice of a static baseline window to all epochs but that was solved when using the regression-based shown in Fig. 10 c. The scalp topographies for the conventional and regression-based approaches will now be compared as shown in Fig. 11. As can be seen, the regression-based technique displays fewer early conditional differences (about 0.5-1 ms) and higher late conditional differences (approximately 1.1-1.6 ms). Let's examine the estimated impact of the baseline period right now. The beta (β) values, as shown in Fig. 12, are important because they demonstrate how highly predictive the baseline

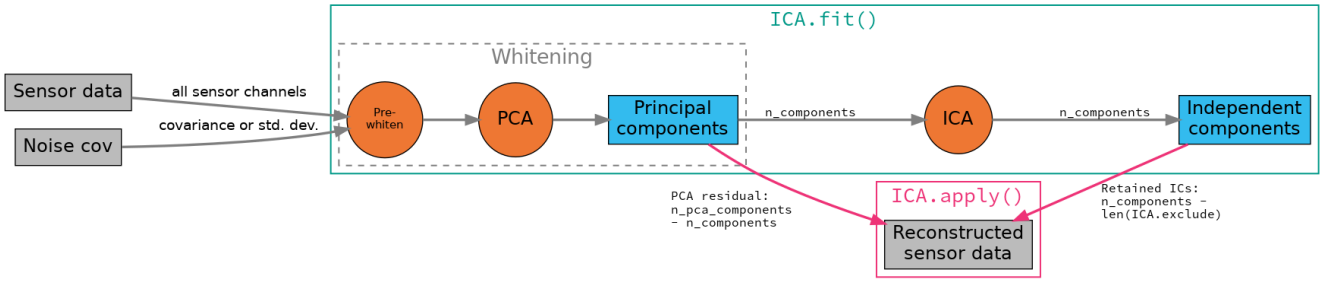

Fig. 7. The fitting and reconstructed process of ICA.

value is at each time point. Unsurprisingly, the pattern shows that the baseline amplitude's predictive value decreases with increasing distance from the baseline period. In other words, the earlier time points (in this data) should have a stronger baseline correction than the later time points.

When classifying the P300 ERP signal for the lying or lying-free group, it was noticed that the P300 of the lying-free group had less amplitude than the lying group, as shown in Fig. 10 c and Fig. 13. Fig. 13 depicts the improvement of the SNR of P300 by the proposed denoising methods.

Table I shows the SNR amount (in dB) for all three stimuli P, T, and I. Based on these results, it was noticed that the SNR of the EEG-ERP signal accompanied by noise (before using any denoising method) was low, but after using the proposed methods, the SNR values increased. To make this increase clearer and include all cases, the mean of all columns in the table was calculated and is mentioned in the last row of the table. As shown in Table I, SNRP refers to the signal-to-noise ratio at the probe stimuli, SNRI is the signal-to-noise ratio at the irrelevant stimuli, and SNRT is the signal-to-noise ratio at the target stimuli.

Using SPSS software to compute paired samples t-test statistical analysis, the significant difference of SNR (as shown in Table I) before and after applying the proposed method to Probe (P), Irrelevant (I), and Target (T) stimuli was evaluated. The $\rho(\text{sig.}) > 0.05$ for all three stimuli indicates the significant difference between SNRs, as shown in Fig. 14.

TABLE I. SNR VALUES BEFORE AND AFTER DENOISING FOR DIFFERENT STIMULI.

Subject	SNRP before	SNRP after	SNRI before	SNRI after	SNRT before	SNRT after
1	7.84	12.58	-2.86	4.22	7.7	11.96
2	-8.54	12	6.98	11.32	-5.74	6.32
3	-10.46	6.1	-10.34	8.54	-0.3	8.88
4	-8.66	-8.14	5.42	7.56	8.3	13.24
5	2.18	7.88	-9.38	-0.2	6.3	15.78
6	1.38	2.5	9.1	12.5	-9.74	3
7	-15.2	6.22	2.9	10.52	-4.2	9.56
8	2.52	8.26	9.2	13.6	2.5	6.9
9	-2.14	-8.76	6.8	10.24	2.9	13.3
10	-12.76	6.22	-1	11.4	-11.08	6.9
Mean	**-4.384**	**4.486**	**1.682**	**8.97**	**-0.336**	**9.584**

Table III shows that this work compares the proposed

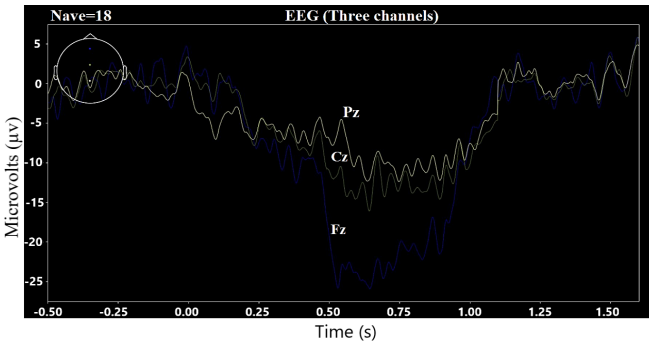

Fig. 8. The difference amplitude between Pz, Cz, and Fz.

method for denoising EEG signals to enhance ERP waveforms with other methods in the literature. Reference [23] used three procedures: Fully Connected Neural Network (FCNN), Recursive Least Squares (RLS) algorithm, and Least Mean Squares (LMS) algorithm. The results discussed the performance of these denoising algorithms in terms of the difference in SNR before and after applying these methods. The highest change in SNR was obtained using the FCNN algorithm.

Reference [16] compared SSP and ICA methods and recommended ICA. However, their results indicated that the value of the SNR achieved was relatively low, as mentioned in Table III.

Reference [24] proposed a deep learning algorithm called "Deep-Separator" to separate noise from EEG signals, reconstruct denoised signals, and extend the approach to multi-channel EEG.

When calculating the increased percentage of mean SNR between the proposed work and the highest-performing method from [**?**], the percentage increase is about 20% (between 8.286 and 9.92) using the following formula:

$$\text{Increase Percentage} = \frac{\text{SNR}_{\text{proposed}} - \text{SNR}_{\text{highest}}}{\text{SNR}_{\text{highest}}} \times 100$$

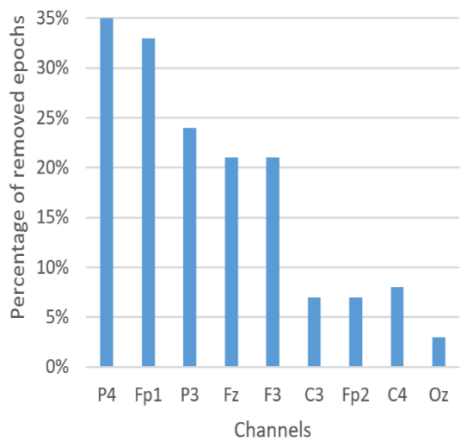

Fig. 9. The percentage of deleted epochs in all EEG-used channels.

where:

$$\mathrm{SNR}_{\mathrm{proposed}} = 8.286, \quad \mathrm{SNR}_{\mathrm{highest}} = 9.92.$$

TABLE II. A COMPARISON OF MEAN (Δ SNR) BEFORE AND AFTER DENOISING.

Reference No.	Method	Mean SNR
[24]	FCNN	8.286
[18]	TSSS	4.1
[25]	Deep Separator	2
Proposed Work	The Proposed Method	9.92

V. CONCLUSION AND DISCUSSION

As mentioned earlier in the results section, the appearance of the ERP-P300 is clearer in the Pz channel for two reasons. First, as shown in Fig. 8, for example, the amplitude of the signal is higher, leading to a more accurate P300 detection. Secondly, the signal in the Pz channel does not exceed $\pm 75\ \mu$V in peak-to-peak amplitude, which means it has a stronger SNR. As shown in Fig. 9, there are no bad epochs in the Pz channel. All of the above aligns with the theories of neurologists, which prove that the location of the Pz channel is responsible for processing attention and memory-related tasks, making it more likely to elicit a clear and strong P300 response during relevant cognitive processes [25].

In this work, the SNR was affected by several factors, including eye movement or blinking of the subject during the data acquisition process. This effect was reduced by using ICA. Another factor was the biasing that occurs in the signal, which leads to distortion of the ERP readings. This problem was solved by using the regression-based baseline correction,

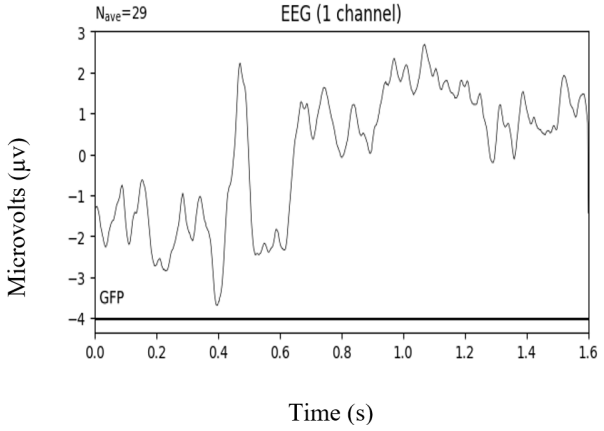

(a) The percentage of deleted epochs in all EEG-used channels.

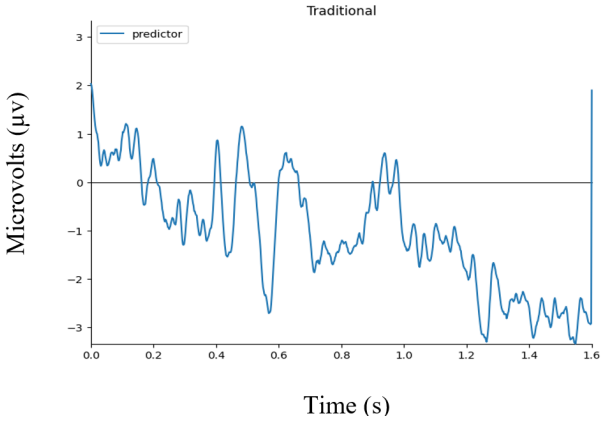

(b) The percentage of deleted epochs in all EEG-used channels.

Fig. 10. (a) The percentage of deleted epochs in all EEG-used channels. (b) The percentage of deleted epochs in all EEG-used channels.

which determines the baseline interval by re-running it for each epoch, differing from the traditional baseline correction method that does not significantly change the biasing state as shown in Fig. 10 (b). These two factors increased the SNR values for the three stimuli P, I, and T, as clearly observed in the "Mean" row in Table I or Fig .14 , as mentioned in the results section.

In this work, the processing time for ten subjects (each having 30 iterations for 5 sessions) did not exceed 10 minutes and did not require high-performance devices. Any laptop with at least 4GB of RAM and Python platform version 3 or higher is sufficient for this work. In contrast, other proposed methods require high-performance devices to run deep learning algorithms. This results in lower costs and less time to execute the required P300 signal preprocessing.

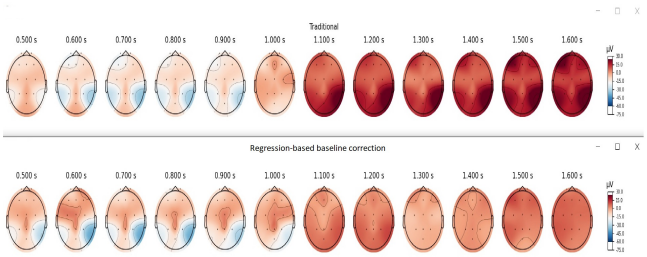

Fig. 11. Scalp topographies of traditional and regression-based methods.

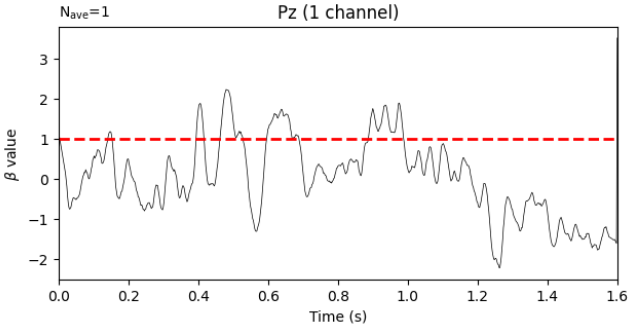

Fig. 12. Baseline regressor and the (β) value.

Conflict of Interest

The authors have declared no conflict of interest.

References

[1] P. Wolpe, K. Foster, and D. LangLeben, "Emerging neurotechnology for lie-detection: Promises and perils," *The American Journal of Bioethics*, vol. 8, no. 2, pp. 520–531, 2001.

[2] A. Bablani, D. Reddy, and V. Kuppili, "Deceit identification test on eeg data using deep belief network," in *IEEE International Conference on Computing and Networking Technology*, pp. 1–4, 2018.

[3] M. Affan, J. Can, and K. George, "Deep learning applications in brain-computer interface based lie detection," in *IEEE 13th Annual Computing and Communication Workshop and Conference*, pp. 189–192, 2023.

[4] S. Ji and et al, "Suicidal ideation detection: a review of machine learning methods and applications," *IEEE Transactions on Computational Social Systems*, vol. 8, no. 1, pp. 214–226, 2021.

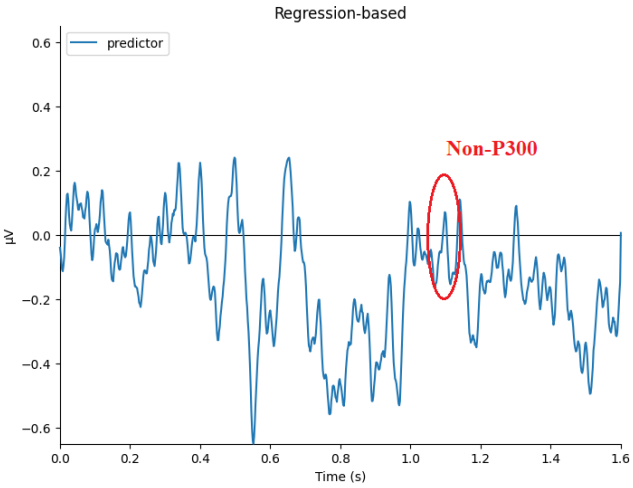

Fig. 13. ERP P300 signal of the lying-free group.

		Paired Differences					t	df	(p) Sig. (2-tailed)
		Mean	Std. Deviation	Std. Error Mean	95% Confidence Interval of the Difference Lower	Upper			
Pair 1	SNR of probe-before & after denoising	-4.43200	4.89139	1.54679	-7.93109	-.93291	-2.865	9	0.019
Pair 2	SNR of irrelevant-before & after denoising	-3.64400	2.56869	0.81229	-5.48153	-1.80647	-4.486	9	0.002
Pair 3	SNR of target-before denoising	-3.76500	3.09660	0.97923	-5.98017	-1.54983	-3.845	9	0.004

Fig. 14. Paired Sample T-Test Result.

[5] Z. Hu, Y. Xia, and J. Xiong, "Lie detection based on a difcw radar with machine learning," in *IEEE MTT-S International Wireless Symposium*, pp. 1–3, 2021.

[6] N. Baghel, D. Singh, M. Kishore, R. Burget, and V. Myska, "Truth identification from eeg signal by using convolution neural network: Lie detection," in *IEEE International Conference on Telecommunications and Signal Processing*, pp. 550–553, 2020.

[7] J. P. Rosenfeld, "P300 in detecting concealed information and deception: A review," *Psychophysiology*, vol. 57, 2020.

[8] J. P. Rosenfeld and et al, "The complex trial protocol (ctp): A new, countermeasure-resistant, accurate, p300-based method for detection of concealed information," *Psychophysiology*, vol. 45, pp. 906–919, 2008.

[9] S. Dodia, D. R. Edla, A. Bablani, and R. Cheruku, "Lie detection using extreme learning machine: A concealed information test based on short-time fourier transform and binary bat optimization using a novel fitness function," *Computational Intelligence*, vol. 36, pp. 637–658, 2019.

[10] Satyender, S. Kumar, and K. Kant, "Eeg artifact removal using canonical correlation analysis and emd-dfa based hybrid denoising approach," *Procedia Computer Science*, vol. 218, pp. 2081–2090, 2023.

[11] P. Alday, "How much baseline correction do we need in erp research? extended glm model can replace baseline correction while lifting its limits," *Psychophysiology*, vol. 56, p. e13451, 2019.

[12] K. Kotowski, J. Ochab, K. Stapor, and W. Sommer, "The importance of ocular artifact removal in single-trial erp analysis: The case of the n250 in face learning," *Biomedical Signal Processing and Control*, vol. 79, 2023.

[13] P. Ablin, J. Cardoso, and A. Gramfort, "Faster independent component analysis by preconditioning with hessian approximations," *IEEE Transactions on Signal Processing*, vol. 66, no. 15, pp. 4040–4049, 2018.

[14] A. Al-Saegh, "Comparison of complex-valued independent component analysis algorithms for eeg data," *Iraqi Journal for Electrical and Electronic Engineering*, vol. 15, 2019.

[15] G. Czanner and et al, "Measuring the signal-to-noise ratio of a neuron," *Proceedings of the National Academy of Sciences*, vol. 112, pp. 7141–7146, 2015.

[16] A. Gonzalez-Moreno and et al, "Signal-to-noise ratio of the meg signal after preprocessing," *Journal of Neuroscience Methods*, vol. 222, pp. 56–61, 2014.

[17] Q. Kang and et al, "Exploring the functional brain network of deception in source-level eeg via partial mutual information," *Electronics*, vol. 12, 2023.

[18] R. Mckearney, S. Bell, M. Chesnaye, and D. Simpson, "Optimizing weighted averaging for auditory brainstem response detection," *Biomedical Signal Processing and Control*, vol. 83, 2023.

[19] Larson and et al, "Mne-python (v1.3.1)." https://zenodo.org/record/2023, 2023. Zenodo.

[20] N. Trusbak, L. Parkkonen, M. Kliuchko, P. Vuust, and E. Brattico, "Comparing the performance of popular meg/eeg artifact correction methods in an evoked-response study," *Computational Intelligence and Neuroscience*, vol. 2016, 2016.

[21] Y. Wan, Y. Zhou, and Z. Yang, "Blind source separation of fast ica algorithm based on negentropy and its optimization," in *Proceedings of SPIE*, vol. 12597, 2023.

[22] A. Li and et al, "Mne-ica label: Automatically annotating ica components with ic label in python," *The Journal of Open Source Software*, vol. 4484, 2022.

[23] I. A. Imran and M. Rabbani, "Comparison of deep learning & adaptive algorithm performance for de-noising eeg," *Journal of Physics: Conference Series*, vol. 2325, 2022.

[24] J. Yu, C. Li, K. Lou, C. Wei, and Q. Liu, "Embedding decomposition for artifacts removal in eeg signals," *Journal of Neural Engineering*, vol. 19, 2022.

[25] J. Polich, "Neuropsychology of p300," in *The Oxford Handbook of Event-Related Potential Components*, pp. 159–188, 2012.